# Mechanisms of Solvent Shifts, Pressure Shifts, and Inhomogeneous Broadening of the Optical Spectra of Dyes in Liquids and Low-Temperature Glasses

**Indrek Renge**

*Physical Chemistry Laboratory, Swiss Federal Institute of Technology (ETH-Zentrum), CH-8092, Zürich, Switzerland*

*Received: January 13, 2000; In Final Form: April 21, 2000*

Optical absorption spectra were measured in liquid solutions at ambient temperature for comparatively nonpolar chromophores: polymethine dyes, polycyclic hydrocarbons, and tetrapyrrolic compounds. The analysis of solvent shifts of band maxima as a function of polarity, polarizability, and hydrogen bonding properties of the medium allows one to distinguish several solvent shift mechanisms. Solvent polarizability dependent red shifts are assigned to dispersive interaction. Hypsochromism in the spectra of open chain cyanine dyes and *s*-tetrazine in polar media may be understood in terms of a multipolar reaction field. Blue shifts of the visible bands of anionic dyes, resorufin, and resazurin occur in alcohols due to the hydrogen bonding with the solvent. Both the polar solvation and the H-bonding with water in the center of tetrapyrrolic macrocycle is responsible for the blue shifts of the $S_1-S_0$ band in porphyrins. Inhomogeneous bandwidths were measured in ethanol glass at 6 K. The reason of inhomogeneous broadening is the spread of microscopic solvent shifts in the disordered matrix that can have the same mechanisms as the macroscopic shifts of band maxima. Alternatively, other broadening mechanisms such as the linear Stark effect in the solvent cavity field do not shift the spectral band as a whole. Further, spectral holes were burned in the inhomogeneous $S_1 \leftarrow S_0$ absorption bands in glassy ethanol and the pressure shift coefficients of the holes $d\nu/dP$ were determined using gaseous He as pressure transmitter. $d\nu/dP$ shows a linear dependence on hole burning wavenumber that can be extrapolated to the frequency $\nu_{0(P)}$ where pressure shift disappears. The $\nu_{0(P)}$ values deviate significantly from the actual 0−0 origins of nonsolvated chromophores. The slope of the dependence of $d\nu/dP$ on hole frequency generally differs from the value of $2\beta_T$ ($\beta_T$ is the isothermal compressibility of the matrix), predicted for the dispersive solvent shift. The slopes steeper than $2\beta_T$ were assigned to short-range repulsive forces. The long-range electrostatic interactions must lead to the slope values less than $\beta_T$.

## Introduction

The solvatochromism of organic compounds is traditionally investigated in liquid solvents with different dielectric and chemical properties.[1] The pressure studies on broad band spectra in liquids are less common since optical cells capable of holding pressure of at least several kbar are required.[2−5] By contrast, in low-temperature solids the relatively small pressure of He gas from a bottle (<200 bar) can produce shift and broadening of spectral holes that are conveniently measurable by tunable lasers.[6] The behavior of resonant holes burned over the inhomogeneous band depends on frequency.[7−19] Usually a linear relationship between the pressure ($P$) shift coefficient $d\nu/dP$ and the burning energy holds, and the transition frequency at which the $P$ shift vanishes ($\nu_{0(P)}$) may be found by extrapolation. It follows from simple model considerations, both microscopic[7,9,20] or macroscopic,[21] that $\nu_{0(P)}$ can give the 0−0 frequency of a nonsolvated chromophore $\nu_0$, whereas the slope of the plot is equal to 2-fold isothermal compressibility of the medium $\beta_T$.

Recently, these predictions have been verified for a number of polymers with known low-temperature compressibilities using tetra-*tert*-butylporphyrazine (*t*-Bu-TAP) as a probe.[21] Several $\pi$-electronic chromophores with available vacuum frequencies were measured in a single matrix, poly(methyl methacrylate). As a rule, poor correspondence between $\nu_0$ and $\nu_{0(P)}$ as well as slopes that can be considerably larger than $2\beta_T$ were observed. Such deviations are by no means surprising, since several solvent shift mechanisms can operate simultaneously, each with different distance dependence between the solute and solvent molecules.

As already mentioned in our previous paper,[21] the pressure effects on spectral holes rise the question about the mechanisms of spectral shifts produced by the surrounding matrix. Bearing in mind the distance dependence, the repulsive and dispersive forces and the electrostatic interactions will be distinguished among the intermolecular interactions. The last ones are assumed to be negligible in aliphatic hydrocarbons, and increasing along with the dielectric permittivity ($\epsilon$) of the liquid. Here we use the liquid-phase studies in solvent sets with gradually varying polarities and polarizabilities in order to specify the solvent shift mechanisms.[1,22−24] The shifts of band maxima in *n*-alkanes are applied for the determination of vacuum frequencies of guest molecules.[25−27] The influence of solvent shift mechanisms on inhomogeneous bandwidth will be discussed.[28]

The low temperature properties of solvent glasses are poorly known. Therefore, a single matrix, the ethanol (EtOH) glass was utilized for hole burning studies. In EtOH many compounds are well soluble and show little ionic association or aggregation. The protic nature of the host provides a hole burning mechanism owing to photoinduced rearrangements in the hydrogen bonding network. The main objective of this paper is to understand the frequency dependence of the $P$ induced shifts of spectral holes. The plots of $d\nu/dP$ vs $\nu$ are in most cases perfectly linear with slopes ranging from $1.5 \times 10^{-5}$ to $6 \times 10^{-5}$ bar$^{-1}$ in EtOH. Finally, the published pressure shift data in frozen solvents and proteins[7−19] are reviewed and discussed.

*Permanent Address: Institute of Physics, University of Tartu, Riia 142, EE51014 Tartu, Estonia. Phone: +3727-304800. FAX: +3727-383033. E-mail: renge@fi.tartu.ee.

10.1021/jp000176n CCC: $19.00 
Published on Web 07/22/2000

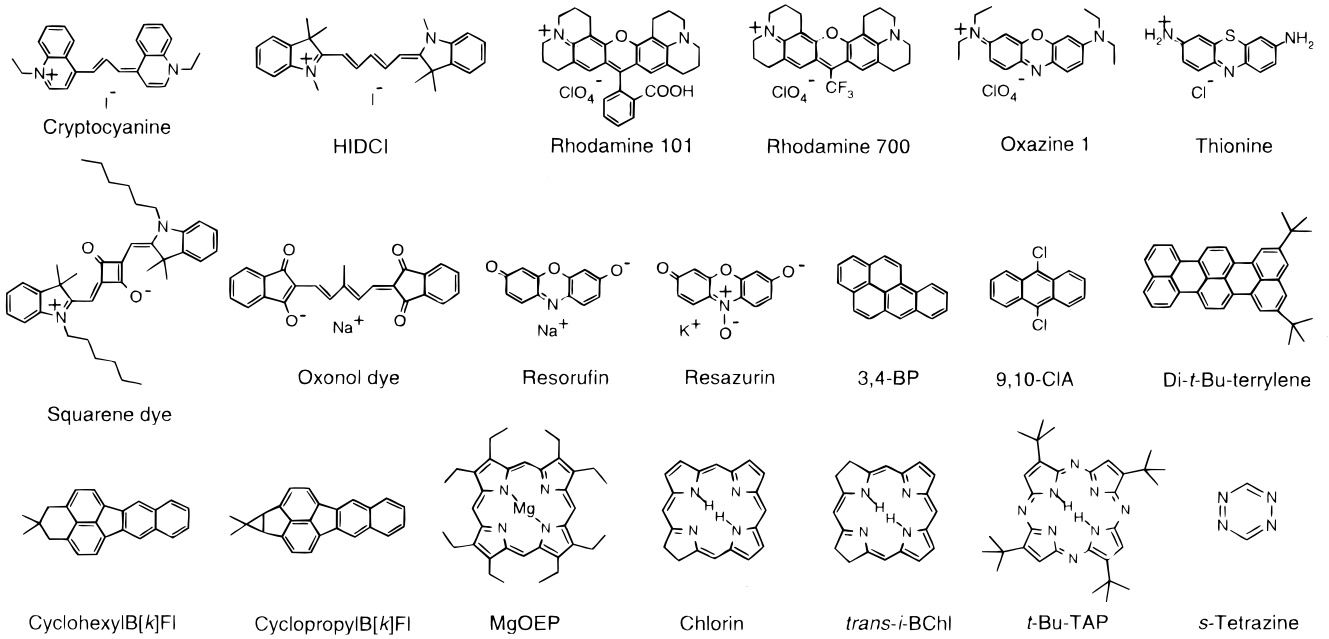


**Figure 1.** Chemical structures of guest molecules.

## Experimental Section

The solvents of highest commercial purity were purchased from Aldrich or Fluka and used as received. The squarene dye was provided by T. L. Tarnowski (Syntex, Palo Alto, CA), chlorin and *iso*-bacteriochlorin by G. Grassi (ETH Zürich), and the benzo[*k*]fluoranthene derivatives by A. Müller (ETH Zürich). Cryptocyanine, 1,1′,3,3,3′,3′-hexamethylindodicarbocyanine iodide (HIDCI), rhodamines 101 and 700, and oxazine 1 were obtained from Lambda Physik, the anionic oxonol dye from the Institute of Dyes (NIIOPiK, Moscow) and the remaining compounds from Aldrich. *s*-Tetrazine was prepared according to ref 29. The chemical structures of guest molecules are depicted in Figure 1.

Absorption spectra were recorded on a Perkin-Elmer Lambda 9 spectrophotometer using the 1−10 mm cells for solutions at room temperature and 0.5−1 mm cells for low-temperature glasses. The hole burning samples were placed in 0.5−1 mm thick open containers made of thin polyethylene film. Pressure shift studies up to 200 bar of He gas pressure were carried out in an optical cell with two 2 mm thick sapphire windows of 4 mm in diameter. The cell body consists of a stainless steel cylinder of 20 mm in diameter housing a sample volume of 2 × 4 × 4 $mm^3$. The sample was cooled as fast as possible by plunging into liquid $N_2$ and loaded in a precooled CF1204 continuous flow cryostat (Oxford). The maximum He gas pressure about 200 bar was applied, the system was let to thermalize during 5 min, and the hole burning was performed between 5 and 8 K. Then the gas bottle valve was closed and the influence of pressure change was followed by releasing the He gas step by step.

Holes were burned with the aid of a Lambda Physik dye laser LPD 3002E pumped with an excimer laser LPX 100. Relatively deep holes broadened by the light dose were created at 3 to 5 positions over the band for a single pressure run. Holes were explored in a two-channel setup using Molectron JD2000 Joulemeter Ratiometer as described previously.[30] The wavelengths ($\lambda$) were converted to wavenumber units ($1/\lambda$, in $cm^{-1}$) as measured, without correction for the refractive index of the air.

**Optical Spectroscopy of Solutions: Model Considerations.** Solvatochromic studies of organic molecules have been dealing predominantly with absorption maxima in liquid solutions at ambient conditions.[1] The method of seeding free large chromophores in cold supersonic jets,[31−34] the studies of frozen solutions by means of spectral hole burning[35] and single molecule spectroscopies,[36] as well as the progress in computational chemistry,[37,38] all stimulate us to take a more detailed approach to the solvent shift problem. Ultimately, one can ask how the spectrum of an individual molecule changes when transferred into a matrix of certain chemical composition and structure and subject to a specified temperature, pressure, external electric field, etc.

The universal, nonspecific interactions may be divided at large into three parts according to their distance dependence: the repulsive interactions, the dispersive interactions, and the phenomena connected with internal fields. The relevance of each mechanism with respect to the pressure-induced hole shifts is shortly described below.

*1. Repulsive Interactions.* The simplest interatomic or intermolecular model potential, the Lennard-Jones formula gives the distance dependencies $r^{-6}$ and $r^{-12}$ for attractive and repulsive energies, respectively. The spectral blue shifts in atomic solids, e.g., individual Na or Hg atoms dispersed in rare gas matrixes have been assigned to the repulsive interactions that are stronger in the excited state than in the ground state.[39] The increase of polarizability of the excited chromophore ($\alpha_e$), if regarded in terms of an expansion of molecular volume would produce an energy upshift.[40] Although in aromatic compounds the $\alpha_e$ can be much larger than the ground-state polarizability ($\alpha_g$),[23] the pressure induced hypsochromism is rarely observed, e.g., for the $^1L_b$ transition of benzene and chlorobenzene in liquid perfluoro-*n*-hexane.[3]

On the other hand, progressive bathochromic shifts take place at very high pressures, revealing no hint to the above-mentioned blue shift of repulsive origin.[4,41] According to Bakshiev formula (see below, eq 4),[22] both the Lorentz−Lorenz equation $\phi(n^2)$ and the Onsager volume depend on matrix compression. Therefore, the linearity of a plot of pressure shift vs the squared relative density of the matrix is expected. Such dependencies

have been built, e.g., for anthracene absorption in PMMA (ref 4, Figure 8) or emission in biphenyl, naphthalen,e and *p*-terphenyl crystals (ref 41, Figure 6) at room temperature and pressures up to 40 kbar. These plots are slightly curved downward demonstrating that either repulsive interactions can cause a red shift or additional bathochromic mechanisms exist at high compressions due to partial solute−solvent electron transfer or electron delocalization in the excited state (the exciplex phenomenon).[41]

Let us assume that the solvent shift defined as a difference between the repulsion energies in the ground and the excited states obeys a similar dependence as the intermolecular repulsive potential in the ground state, $r^{-12}$. Then the pressure shift can be expressed in terms of isothermal compressibility of the medium $\beta_T$ ($\beta_T = -(\mathrm{d}V/\mathrm{d}P)_T V^{-1}$) and the solvent shift ($\nu_{\mathrm{rep}} - \nu_0$) as[21]

$$\mathrm{d}\nu_{\mathrm{rep}}/\mathrm{d}P = 4\beta_T(\nu_{\mathrm{rep}} - \nu_0) \tag{1}$$

*2. Dispersive Interaction.* Large red shifts of the optical bands of nonpolar solutes in nonpolar solvents are ascribed to the attractive London forces. Longuet-Higgins and Pople deduced an approximate microscopic formula for this shift using perturbation theory:[42]

$$\Delta\nu_{\mathrm{disp}} = 1/6\alpha_s z\bar{r}^{-6}(1/4\nu_0\alpha_g + f^2) \tag{2}$$

where $\alpha_s$ is the solvent polarizability, $z$ is the number of surrounding solvent molecules placed at an average distance $\bar{r}$, $\nu_0$ is the transition energy of free solute, and $f$ is the oscillator strength. Instead of $\alpha_s$, $z$, and $r$, the refractive index ($n$) function of the bulk solvent $\phi(n^2)$ can be used, according to the Lorentz−Lorenz equation:[43]

$$\phi(n^2) = (n^2 - 1)/(n^2 + 2) \tag{3}$$

We have demonstrated that the shifts of optical transitions of very different intensities in tetrapyrrolic pigments dissolved in liquid *n*-alkanes cannot be well described with experimentally easily accessible $\nu_0$ and $f$.[26]

The Bakhshiev equation that uses the polarizability difference between the ground and the excited state has proved more successful:[22−27]

$$\Delta\nu_{\mathrm{disp}} = \nu_0 + p\phi(n^2)$$
$$p = -3II'(\alpha_e - \alpha_g)/[2(I + I')r^3] \tag{4}$$

where $I$ and $I'$ are the ionization energies of the solute and solvent molecules and $r$ is the Onsager cavity radius.

Concerning the bandwidths at low temperatures, it has been estimated that the width of the inhomogeneous site distribution function (IDF) is about 10% of the dispersive solvent shift (plus a residual value of ∼100 $\mathrm{cm}^{-1}$) in solvent glasses.[28] This is undoubtedly related to the fact that glasses contain approximately 10% of free space that corresponds on the average to a single vacancy among ∼10 solvent molecules in the closest coordination layer of the solute.

Since the Lorentz−Lorenz function and $r^{-3}$ both increase upon compression of the matrix, the pressure shift of spectral holes may be expressed in terms of isothermal compressibility of the medium $\beta_T$:[21]

$$\mathrm{d}\nu_{\mathrm{disp}}/\mathrm{d}P = 2\beta_T(\nu_{\mathrm{disp}} - \nu_0) \tag{5}$$

*3. Internal Electric Field Effects.* General theory of shifts and broadening of electronic spectra of polar solutes in polar media have been developed by R. Marcus, who presented also an analysis of earlier work.[44] In an ideal case, the electric field $E$ of a cavity formed in a polar host matrix is treated as homogeneus but, of course, of fluctuating magnitude and direction. It can produce both linear and quadratic Stark effects on impurity spectra:

$$\Delta\nu = \Delta\mu E\cos\varphi + 1/2\Delta\alpha E^2 \tag{6}$$

where $\Delta\mu$ is the dipole moment difference between the ground and the excited state and $\varphi$ is the angle between $\Delta\mu$ and $E$. Because the vectors $\Delta\mu$ and $E$ are oriented randomly, no shift of the band maximum is expected for the linear effect in the cavity field.

Another field is formed if the solute molecule has a dipole moment in the ground state ($\mu_g$). Energetically more favorable mutual orientations of the guest and host molecules gain more statistical weight producing an average reaction field that is collinear with $\mu_g$. The interaction of this field with the vector difference $\Delta\mu$ leads to a net transition frequency shift that can be both to the blue or to the red, depending on the magnitude and mutual orientation of the ground and the excited-state dipole moments ($\mu_e$):[22]

$$\Delta\nu_{\mathrm{Stark1}} = \mu_g(\mu_g - \mu_e\cos\gamma)[\phi(\epsilon) - \phi(n^2)]/r^3 \tag{7}$$

where $\gamma$ is the angle between $\mu_g$ and $\mu_e$, $\phi(\epsilon) = (\epsilon - 1)/(\epsilon + 2)$, and $\epsilon$ is dielectric constant. Equation 7 is valid in fluids where the dipoles are free to move.

It follows from eq 7 that the pressure shift in liquids is $2\beta_T$ times of the solvent shift, since both $\phi(\epsilon) - \phi(n^2)$ and $r^{-3}$ are inversely proportional to the volume. By contrast, in the solid phase the static field scales proportionally with linear compressibility of the matrix $\alpha_T$ ($\alpha_T = 1/3\beta_T$). Therefore, for the $P$ induced shift of spectral holes, one obtains:

$$\mathrm{d}\nu_{\mathrm{Stark1}}/\mathrm{d}P = 1/3\beta_T(\nu_{\mathrm{Stark1}} - \nu_0) \tag{8}$$

In centrosymmetric chromophores the linear Stark effect vanishes ($\Delta\mu = 0$). For the quadratic Stark shift,[45] empirical relationships have been found with the polarizability difference of the chromophore $\Delta\alpha$ and the dielectric permittivity function of the solvent $\phi(\epsilon) - \phi(n^2)$.[24] However, it has been noticed that very intense $\beta$ (or $^1B_b$) transitions in polycyclic hydrocarbons shift weakly between a nonpolar and a polar solvent of similar refractive index,[46] despite the $\Delta\alpha$ values as large as 35 Å$^3$.[23] This rises a question whether the quadratic Stark effect in the solvent cavity field is real. As an alternative explanation, a theory of solute quadrupole-solvent dipole interactions has been advanced.[46] A solvent shift equation similar to eq 7 was obtained:

$$\Delta\nu_{\mathrm{quadru}} = Q_g(Q_g - Q_e)[\phi(\epsilon) - \phi(n^2)]/r^5 \tag{9}$$

where $Q_g$ and $Q_e$ are the quadrupole moments of the solute in the ground and the excited state, respectively. The distance dependence of $\Delta\nu_{\mathrm{quadru}}$ is stronger than that for dipolar reaction field (eq 7). Perhaps the matrix compression effect on hole shift in a frozen glass would be stronger too, at least by a factor of $r^{-2}$ resulting in an increase of the pressure sensitivity from $1/3\beta_T$ (linear Stark effect, eq 8) to $\beta_T$.

The bandwidths remain broad at low temperatures, since the fluctuating internal fields are rendered static upon solidification

of the glass. Approximately, the Stark shifts and the width of IDF are of comparable magnitude in polar systems, e.g., 500 $cm^{-1}$ for 9-cyanoanthracene in propylene carbonate glass.[28] Although the local electric field phenomena are still disputable topics, it is evident that for not very polar chromophores (not a charge-transfer transition) the fields produce a relatively small displacement of band maxima and a weak frequency dependence of pressure shift coefficients (less than $\beta_T$) but much inhomogeneity of spectra.[28]

Therefore, following the arguments of this section the total shift of a zero-phonon hole from the 0−0 origin of a free chromophore may be split into following components:

$$\Delta\nu = \Delta\nu_{rep} + \Delta\nu_{disp} + \Delta\nu_{Stark1} + \Delta\nu_{Stark2} + \Delta\nu_{quadru} \quad (10)$$

The pressure induced shift of spectral holes depends on the magnitudes of respective solvent shift components and the volume compressibility of the host matrix:

$$d\nu/dP = (4\Delta\nu_{rep} + 2\Delta\nu_{disp} + 1/3\Delta\nu_{Stark1} + 2/3\Delta\nu_{Stark2} + \Delta\nu_{quadru})\beta_T \quad (11)$$

## Results and Discussion

**1. Solvent Shift Mechanisms.** The selection of chromophores with strong phononless transitions is limited to relatively nonpolar ones, since extensive charge redistribution upon electronic excitation dramatically enhances both the Franck−Condon coupling to molecular vibrations and the Debye−Waller coupling to matrix modes.[47] The solutes are grouped according to the effective dimensionality of the $\pi$-electronic system: linear (polymethines) and planar (polyarenes, tetrapyrroles, and a n−$\pi$* chromophore, *s*-tetrazine). Compounds with weak $S_1$ transitions, linear polyenes, and three-dimensional fullerenes were not studied. The nonspecific (refractive index *n* and dielectric permittivity $\epsilon$) and the specific solvation parameters (nucleophilicity *B* and electrophilicity *E* after Koppel and Palm[1,48]) of solvents are collected in Table 1.

Room-temperature spectra of neutral compounds were recorded in *n*-alkanes. Because the electronic polarization of the solvent with solute dipole moments is small in our chromophores,[22] the refractive index (*n*) dependence of absorption band maxima $\nu_{max}$ is of dispersive origin. The plots of band maxima in *n*-alkanes vs the Lorentz−Lorenz function $\phi(n^2)$ (eq 3) are perfectly linear with correlation coefficients larger than 0.99 (Table 2). Both the $\nu_0$ and the polarizability difference can be estimated from the intercept and the slope (*p*, further on referred to as Bakshiev number) of eq 4, respectively.[22,23,25]

For ionic compounds that are insoluble in hydrocarbons a set of highly polar aprotic solvents with gradually changing *n* from acetonitrile to nitrobenzene was applied (Table 1).[25] In this case the correlation coefficient is lower and the vacuum frequency should be corrected for the dielectric shift (Table 2).[25] For the neutral squarene dye, both the *n*-alkane and polar series yield $\nu_0$ values within 100 $cm^{-1}$, whereas the Bakhshiev numbers are slightly different: $-2617 \pm 84$ and $-3137 \pm 346$ $cm^{-1}$, respectively (Table 2). The effects of polarity can be documented separately in solvents with approximately constant *n*, while changing the dielectric permittivity $\epsilon$ (e.g., from $CHCl_3$ to propylene carbonate).[25]

*1. Polymethines*. Dyes with similar length of polymethine chain were chosen in this work: the 9 atom chains (including terminal heteroatoms) in cryptocyanine, HIDCI, and the squarene dye and the 11 atom chains in the remaining compounds. Accordingly, the $S_1-S_0$ transition energies of nonsolvated dyes

**TABLE 1: Properties of the Solvents at 293 K[a]**

| symbol | solvent | *n* | $\phi(n^2)$ | $\epsilon$ | $\phi(\epsilon)$-$\phi(n^2)$ | *B* | *E* |
|---|---|---|---|---|---|---|---|
| | Nonpolar Solvents Other Than *n*-Alkanes | | | | | | |
| a | perfluoro-*n*-octane | 1.3000 | 0.187 | | | | |
| b | dioxane | 1.4220 | 0.254 | 2.27 | 0.039 | 237 | 4.2 |
| c | carbon tetrachloride | 1.4600 | 0.2739 | 2.30 | 0.028 | (0) | (0) |
| d | toluene | 1.4960 | 0.292 | 2.43 | 0.031 | 58 | 1.3 |
| e | benzene | 1.5010 | 0.295 | 2.40 | 0.023 | 48 | 2.1 |
| f | hexachlorobutadiene | 1.5550 | 0.321 | 2.59 | 0.025 | | |
| g | carbon disulfide | 1.6270 | 0.3544 | 2.64 | 0.00 | | (0) |
| | Less Polar ($\epsilon$ < 30) Aprotic Solvents | | | | | | |
| 1 | diethyl ether | 1.3526 | 0.2166 | 4.42 | 0.316 | 280 | (0) |
| 2 | acetone | 1.3588 | 0.220 | 21.36 | 0.652 | 224 | 2.1 |
| 3 | methyl acetate | 1.3593 | 0.2203 | 6.94 | 0.444 | 181 | |
| 4 | triethylamine | 1.4000 | 0.2424 | 2.45 | 0.083 | 650 | (0) |
| 5 | tetrahydrofuran | 1.4035 | 0.244 | 7.47 | 0.437 | 287 | (0) |
| 6 | 2-methyltetra-hydrofuran | 1.4060 | 0.2456 | | | | |
| 7 | bromoethane | 1.4235 | 0.2549 | 9.59 | 0.486 | | |
| 8 | dichloromethane | 1.424 | 0.2552 | 8.9 | 0.470 | 23 | 2.7 |
| 9 | 1-bromopropane | 1.4336 | 0.2602 | 8.44 | 0.452 | | |
| 10 | cyclopentanone | 1.437 | 0.2620 | 14.45 | 0.556 | | |
| 11 | epichlorhydrin | 1.438 | 0.2625 | 22.6 | 0.616 | | |
| 12 | 1,2-dichloroethane | 1.445 | 0.2662 | 10.74 | 0.498 | 40 | 3.0 |
| 13 | chloroform | 1.446 | 0.2667 | 4.89 | 0.298 | 14 | 3.28 |
| 14 | ethyl trichloroacetate | 1.4500 | 0.269 | 9.03 | 0.459 | | |
| 15 | pyridine | 1.510 | 0.2991 | 13.55 | 0.508 | 472 | (0) |
| 16 | benzonitrile | 1.528 | 0.3079 | 25.30 | 0.582 | 155 | (0) |
| 17 | iodomethane | 1.531 | 0.3094 | 6.92 | 0.354 | | |
| 18 | bromoform | 1.5960 | 0.3403 | 4.39 | 0.190 | | |
| | Highly Polar ($\epsilon$ > 30) Aprotic Solvents | | | | | | |
| A | acetonitrile | 1.3441 | 0.2119 | 36.00 | 0.709 | 160 | 5.2 |
| B | nitromethane | 1.3817 | 0.233 | 36.16 | 0.688 | 65 | 5.1 |
| C | propylene carbonate | 1.4189 | 0.252 | 62.93 | 0.702 | | |
| D | *N*,*N*-dimethyl-formamide | 1.431 | 0.2588 | 37.06 | 0.664 | 291 | 2.6 |
| E | $\gamma$-butyrolactone | 1.4365 | 0.262 | 40.96 | 0.668 | | |
| F | dimethylsulfoxide | 1.479 | 0.2836 | 46.71 | 0.655 | 362 | 3.2 |
| G | sulfolane | 1.4840 | 0.286 | 42.13[b] | 0.646 | 157 | 2.3 |
| H | furfural | 1.5262 | 0.307 | 42.1 | 0.625 | | |
| I | nitrobenzene | 1.5562 | 0.322 | 36.09 | 0.599 | 67 | (0) |
| | Protic Solvents | | | | | | |
| $\alpha$ | methanol | 1.329 | 0.2034 | 33.52 | 0.712 | 218 | 14.9 |
| $\beta$ | water | 1.3330[c] | 0.2057 | 81.2 | 0.758 | 156 | 21.8 |
| $\delta$ | ethanol | 1.360 | 0.2207 | 25.3 | 0.669 | 235 | 11.6 |
| $\epsilon$ | *N*-methylformamide | 1.4320 | 0.2594 | 189.5 | 0.725 | 287 | 11.9 |
| $\phi$ | *N*-methylacetamide | 1.4330 | 0.260 | 178.9[d] | 0.723 | | |
| $\gamma$ | formamide | 1.447 | 0.2672 | 111.8 | 0.706 | 270 | 14.5 |

[a] *n*, refractive index for Na D line from ref 49; $\phi(n^2) = (n^2 - 1)/(n^2 + 2)$; $\epsilon$, dielectric constant from refs 50 and 51; $\phi(\epsilon) = (\epsilon - 1)/(\epsilon + 2)$; *B* and *E*, general basicity and acidity parameters, respectively, from refs 1 and 49. [b] At 30 °C. [c] Reference 52. [d] At 25 °C.

$\nu_0$ are rather close (between 15000 and 18000 $cm^{-1}$). The Bakhshiev numbers (and the polarizability differences between the ground and the excited state)[22,23] show also little variation ($p = -3000 \pm 500$ $cm^{-1}$, Table 2).

Several structural features leading to the deviation of the $S_1$ transition energy from the "electrons in the one-dimensional box" model become obvious in the investigated set of dyes (Figure 1). The presence of $\pi$-electronic loops increases the effective length of the chain that results in the downshift of $\nu_0$ in cryptocyanine. Bending of the conjugated system produces an energy upshift (rhodamine 101, resorufin). Electron withdrawing substitution at the chain center in cations (N atom at the middle ring of oxazin 1, $-CF_3$ in rhodamine 700) causes a red shift.

Although the solvent polarizability effect is rather uniform in polymethines, the influence of polarity and protic character on band maxima and widths is variable. In highly polar solvents the $S_1-S_0$ bands of rhodamine 700 (Figure 2b), resorufin (Figure 2f) and oxazine 1 undergo a bathochromic shift, whereas the

**TABLE 2: Solvent Shift Parameters of Dopants at 293 K[a]**

| dopant | $\nu_0$(cm$^{-1}$) | $\Delta\nu'$(cm$^{-1}$) | $\nu_0'$(cm$^{-1}$) | $-p$(cm$^{-1}$) | $N$ | $r$ | solvents[b] |
|---|---|---|---|---|---|---|---|
| **Polymethine Compounds** | | | | | | | |
| pseudoisocyanine $I^-$[c] | 19716 ± 40 | | | 2964 ± 147 | 31 | 0.966 | |
| cryptocyanine $I^-$ | 14833 ± 75 | −200 | 14630 | 3024 ± 286 | 8 | 0.974 | A−H |
| HIDC $I^-$ | 16357 ± 63 | −300 | 16060 | 3156 ± 241 | 8 | 0.983 | A−H |
| rhodamine 101 $ClO_4^-$[d] | 17995 ± 66 | | | 3027 ± 245 | 7 | 0.984 | A−C,E,G−I |
| rhodamine 700 $ClO_4^-$[d] | 16027 ± 32 | 200 | 16230 | 2577 ± 120 | 7 | 0.9947 | A−E,G−I |
| oxazine 1 $ClO_4^-$[d] | 16091 ± 76 | 50 | 16140 | 2782 ± 278 | 8 | 0.971 | A−C,E−I |
| thionine $Cl^-$ | 17684 ± 184 | 100 | 17780 | 3680 ± 681 | 7 | 0.924 | A−C,E,G−I |
| squarene dye | 16353 ± 20 | | | 2617 ± 84 | 7 | 0.9969 | $C_5$−$C_{10}$,$C_{16}$ |
| | 16437 ± 93 | | | 3137 ± 346 | 8 | 0.965 | A−F,H,I |
| oxonol dye $Na^+$ | 15543 ± 75 | −200 | 15340 | 3634 ± 274 | 8 | 0.983 | A−C,E−I |
| resorufin $Na^+$ | 17535 ± 130 | 50 | 17590 | 2435 ± 481 | 9 | 0.886 | A−I |
| resazurin $K^+$ | 16192 ± 218 | | | 1594 ± 831 | 9 | 0.587 | 2,6,15,A−D,F,I |
| **Polycyclic Aromatic Hydrocarbons** | | | | | | | |
| 3,4-benzopyrene[d] | 25202 ± 15 | | | 1567 ± 60 | 4 | 0.999 | |
| | 25265[e,f] | | | | | | |
| 9,10-dichloroanthracene | 25950[e,g] | | | 4175[d,h] | | | |
| di-*tert*-butylterrylene | 19213 ± 54 | | | 4983 ± 224 | 8 | 0.9940 | $C_5$−$C_{10}$,$C_{13}$,$C_{16}$ |
| benzo[*k*]fluoranthene | 25637 ± 19 | | | 3016 ± 81 | 6 | 0.9986 | $C_5$−$C_8$,$C_{11}$,$C_{16}$ |
| **Tetrapyrrolic Compounds** | | | | | | | |
| Mg octaethylporphine | | | | 601 ± 15[i] | | | |
| chlorin[d] | 15857 ± 5 | | | 659 ± 20 | 3 | 0.999 | |
| | 15912[e,j] | | | | | | |
| *trans-iso*-bacteriochlorin | 17985 ± 11 | | | 2176 ± 46 | 6 | 0.9991 | $C_5$−$C_8$,$C_{11}$,$C_{16}$ |
| tetra-*tert*-butylporphyrazine | 16326 ± 9 | | | 988 ± 39 | 7 | 0.9961 | $C_5$−$C_9$,$C_{11}$,$C_{16}$ |
| **Azaarenes with n-$\pi^*$ Transitions** | | | | | | | |
| tetrazine | 18158 ± 6 | | | 1062 ± 23 | 7 | 0.9989 | $C_5$−$C_8$,$C_{10}$,$C_{14}$,$C_{16}$ |
| | 18128[e,k] | | | | | | |

[a] $\nu_0$, extrapolated transition frequency in a vacuum, eq 4; $\Delta\nu'$, polarity correction factor; $\nu_0'$, corrected value of $\nu_0$; $p$, Bakshiev number (slope of the solvatochromic plot, eq 4); $N$, number of data points; $r$, correlation coefficient. [b] $C_5$−$C_{16}$, *n*-alkanes from *n*-pentane to *n*-hexadecane, other solvents are denoted as in Table 1. [c] In 50% (w/w) glycerol/water, ref 53. [d] Reference 25. [e] In supersonic jet. [f] Reference 31. [g] Reference 32. [h] For anthracene. [i] For Zn octaethylporphine, ref 26. [j] Reference 33. [k] Reference 34.

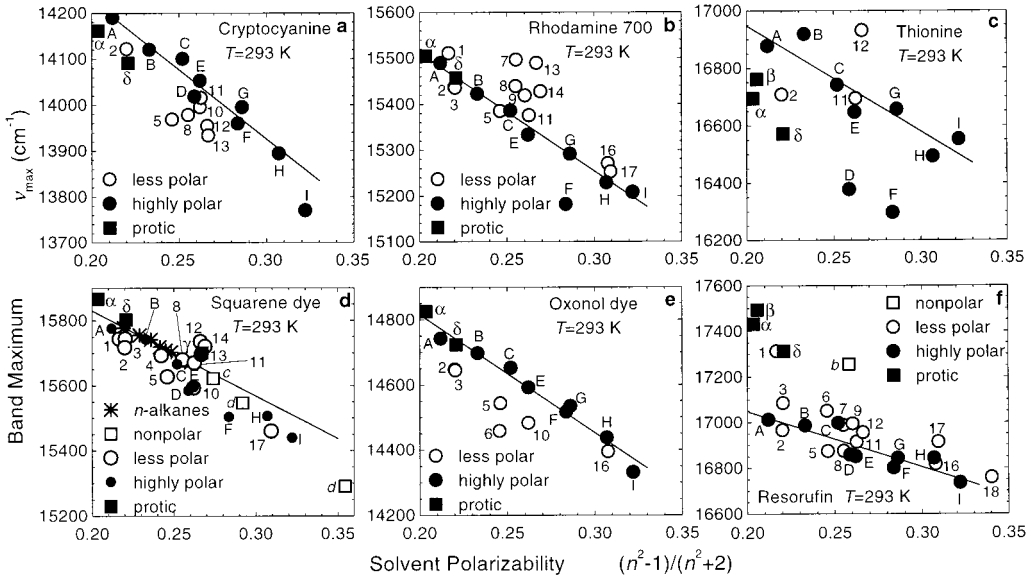


**Figure 2.** Dependence of $S_1$ absorption band maxima of polymethine dyes on the Lorentz−Lorenz function of solvents at room temperature. Solvents are denoted as in Table 1. Linear regression lines are shown for *n*-alkanes (squarene dye) or highly polar aprotic solvents. The fitting parameters are collected in Table 2.

open-chain structures, both cationic (HIDCI, cryptocyanine, Figure 2a) and anionic (oxonol, Figure 2e), show hypsochromic displacement. The bathochromic shift in rhodamines may be caused by a reaction field created with a permanent dipole moment in a polar environment (eq 7). Rhodamines probably possess an appreciable dipole moment, since for rhodamine 6G the difference between $\mu_g$ and $\mu_e$ as large as 4.6 D has been reported.[54]

As for the hypsochromism of open-chain cyanines and oxonols in polar media (Figure 2a and e), no theoretical relationship has been proposed. The partial charges on polymethine carbon atoms may produce ordering of solvent dipoles that makes up a reaction field of higher multipolar origin (eq 9).[46] Since in the excited state the charges are shifted to the neighboring atoms, an extra energy is needed to carry out work against the existing reaction field.

The influence of hydrogen bonds can be best demonstrated by comparing the protic and aprotic environments with similar

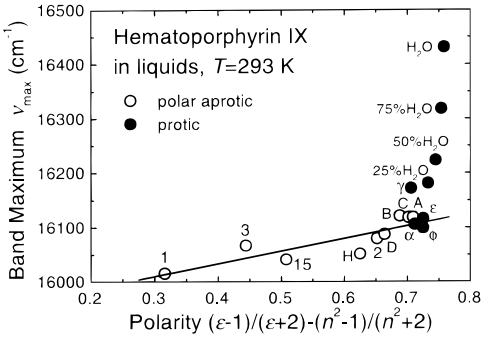


**Figure 3.** Dependence of $S_1$ absorption band maximum of hematoporphyrin IX on solvent polarity function $\phi(\epsilon) - \phi(n^2)$ at room temperature (Table 1). The blue shifted maxima in water, its mixtures with methanol (indicated in v/v %) and formamide are excluded from the regression line (eq 12).

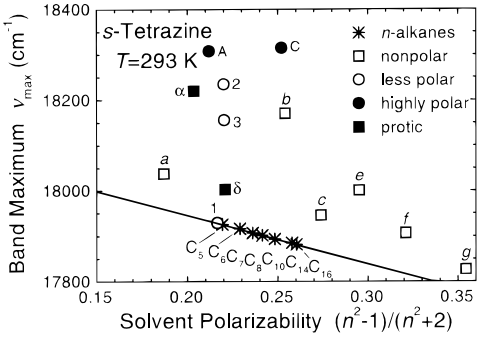


**Figure 4.** Dependence of absorption band maxima of *s*-tetrazine on the Lorentz−Lorenz function of solvents at room temperature. Solvents are denoted as in Table 1. Linear regression line is shown for *n*-alkanes. The fitting parameters are collected in Table 2.

*n* and $\epsilon$, such as methanol and acetonitrile or ethanol and acetone (Figure 2). The effect of H-bondig solvents is negligible in cryptocyanine, HIDCI, rhodamine 700, oxazine 1, the squarene and oxonol dyes. By contrast, a pronounced displacement of band maxima by 300−500 cm$^{-1}$ to the higher energies is observed for cyclic anions, resorufin and resazurin in alcohols. For thionine cation a $\sim -200$ cm$^{-1}$ red shift is measured in alcohols with respect to the solvents of identical *n* and $\epsilon$ (Figure 2c). Also, in strongly nucleophilic media (see the basicity parameters *B* in Table 1), DMF and DMSO (solvents D and F in Figure 2c and Table 1) an extra red shift by $\sim -350$ cm$^{-1}$ is detected for thionine reflecting the complex formation with the dye as a hydrogen bonding donor.

*2. Polyarenes*. Polycyclic aromatic hydrocarbons exhibit presumably the simplest solvatochromic behavior with prevailing dispersive red shift. The Bakshiev number lies in the range of −1000 to −2000 and −4000 to −5000 cm$^{-1}$ for the $^1L_b$ ($\alpha$) and $^1L_a$ (p) types of transitions of alternant hydrocarbons, respectively.[23] In polar media the cavity field produces a red shift with the coefficient $y \sim 0.05p$ per unit polarity function $[\phi(\epsilon)-\phi(n^2)]$ ascribed to the quadratic Stark effect on the solvent cavity field[24,28,45] or, alternatively, to a quadrupolar reaction field effect.[46]

*3. Tetrapyrroles*. In free-base tetrapyrroles the dispersive shift of the first absorption band is small: *p* is equal to −336, −659, and −988 cm$^{-1}$ for porphine,[27] chlorin,[23,25,26] and *t*-Bu-TAP,[27,30] respectively (Table 2). A peculiar hypsochromism of the $S_1$ ($Q_y$) band appears in polar media, while the second band ($Q_x$) undergoes a bathochromic displacement.[26] This phenomenon have been ascribed to the shift of central protons closer to each other in polar environment as a result of a decrease of their mutual electrostatic repulsion.[26]

The influence of pressure on spectral holes burned in the $S_1-S_0$ bands of mesoporphyrin IX[11,13,16] and protoporphyrin IX[10,13−15] in protein complexes has been reported. To understand better the pigment−protein interactions the band maxima were measured for a related pseudo-octaalkylporphine, hematoporphyrin IX in liquids, including water (Figure 3). The increase of solvent (di)polarity produces the characteristic hypsochromic effect also for hematoporphyrin:[26]

$$\nu_{max} = (15940 \pm 26) + (233 \pm 41)[\phi(\epsilon) - \phi(n^2)], \quad N = 12, \quad r = 0.872 \quad (12)$$

More importantly, water causes a huge 260 cm$^{-1}$ blue shift as compared with that in another protic solvent with similar dielectric constant, formamide. Owing to its small size, one or even two $H_2O$ molecules are perhaps able to approach the porphyrin ring and form a bidentate hydrogen bonded complex with its center. Thus, Figure 3 unambiguously demonstrates a prominent solvent shift due to the specific solvation of porphyrins with water.

A reduced porphine, trans-*iso*-bacteriochlorin (trans-*i*-BChl), is characterized by a rather large dispersive effect with $p = -2176$ cm$^{-1}$. More remarkably, there is a bathochromic shift of the $S_1$ band between *n*-pentane and acetonitrile of −250 cm$^{-1}$ that is opposite to the other free-base tetrapyrroles. This anomaly is perhaps connected with central H atoms too, since the dipole moment change of trans-*i*-BChl ($\Delta\mu = 1.64$ D)[55] is likely to be responsible only for a minor reaction field shift.

*4. Azaarenes*. The n−$\pi$* transition in *s*-tetrazine shifts to the red in *n*-alkanes, with Bakhshiev number −1062 ± 23 cm$^{-1}$ (Figure 4). The linear plot of $\nu_{max}$ vs $\phi(n^2)$ yields the extrapolated vacuum frequency of 18158 ± 6 cm$^{-1}$ that is very close to the 0−0 origin of nonsolvated molecule in a supersonic jet (18128 cm$^{-1}$)[34] or in room-temperature vapors (18133.3 cm$^{-1}$, measured in a 10 cm cell). Despite the lack of dipole moment in *s*-tetrazine, the polar solvents cause remarkable hypsochromic deviations from the plot for *n*-alkanes, amounting to 380 cm$^{-1}$ between *n*-pentane and acetonitrile. Quite large extra blue shifts occur also in nonpolar solvents other than *n*-alkanes: dioxane, $CCl_4$, $C_6H_6$, hexachlorobutadiene, and $CS_2$. There is little doubt that multipolar effects are involved, as in the case of cyanines (see above). In protic methanol and ethanol, the hypsochromic effect is reduced by 100−200 cm$^{-1}$ with respect to acetonitrile and acetone, a feature that remains to be explained. As in the case of free-base porphyrins, the strong water anomaly is present in tetrazine consisting of a ∼600 cm$^{-1}$ blue shift of the dramatically broadened band contour relative to the center of spectral envelope in acetonitrile (data not shown).

*5. Solvent shifts in EtOH glass*. The absolute shifts of band maxima in EtOH glass at 6 K may be compared with the shifts in a nonpolar matrix with similar *n* calculated as $p\phi(n^2)$ (Figure 5). The Lorentz−Lorenz function of the glass was assumed to be 0.28, by 25% larger than that of the room-temperature liquid. Polycyclic hydrocarbons 3,4-benzopyrene (3,4-BP), 9,10-dichloroanthracene (9,10-ClA) and di-*t*-Bu-terrylene as well as the squarene dye display nice agreement between the liquid and solid phase data, demonstrating that the matrix shift in EtOH is mainly dispersive.

The polarity induced blue-shift counteracting the polarizability effect is apparent in cryptocyanine (250 cm$^{-1}$), HIDCI (320 cm$^{-1}$), oxonol dye (350 cm$^{-1}$), *t*-Bu-TAP (180 cm$^{-1}$), and *s*-tetrazine (200 and 450 cm$^{-1}$ for two solvate complexes, the latter is upshifted with respect to $\nu_0$ by 160 cm$^{-1}$). These

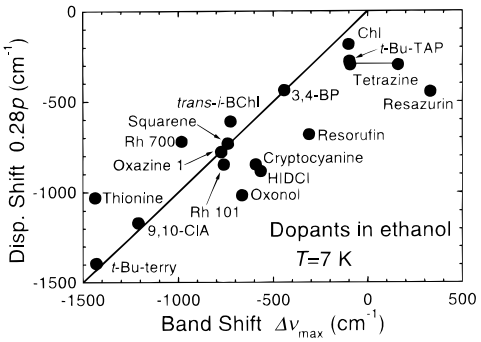


**Figure 5.** Vacuum-to-matrix shifts of band maxima in ethanol glass at 6 K plotted vs the dispersive red-shiftcalculated from the Bakshiev number $p$ and the matrix polarizability $\phi(n^2) = 0.28$. Deviations from the line with unit slope expose the solvent shift mechanisms other than dispersive.

hypsochromic displacements may originate primarily from a quadrupolar reaction field and show up in small pressure shifts of spectral holes (see below). The observed solvent shift is also much less than $0.28p$ in resorufin (by 380 $cm^{-1}$) and resazurin (by 750 $cm^{-1}$) owing to the hydrogen bonding that is particularly strong at low temperatures. In fact, the transition frequency of H-bonded resazurin is by 330 $cm^{-1}$ higher than the predicted vacuum value (Table 3). On the other hand, an extra red shift in solid EtOH occurs in rhodamine 700 ($-250$ $cm^{-1}$) because of its polarity and in thionine ($-420$ $cm^{-1}$) as a result of hydrogen bonding.

**2. Mechanisms of Inhomogeneous Broadening.** The inhomogeneous spread of transition frequencies and the shifts of bands as a whole can have a common microscopic origin. On the other hand, several interactions such as the linear Stark effect in the cavity field are not capable of shifting the band but may produce substantial broadening. A comparison of band broadening with the absolute shifts of maxima is made in this section with the aim to elucidate further the guest−host interactions in glasses.

The 2-fold half-widths at half-maximum of a long-wavelength slope of the band (2hwhm) and the solvent shifts of band maxima in EtOH glass are given in Table 3. The widths of IDF and the Debye−Waller factors were not rigorously measured in this work. Instead, the contribution of phonon sidebands to the measured bandwidth was assessed by comparing the 2hwhm and the full widths at half-maxima (fwhm) (Table 3). The fwhm is considerably broader in HIDCI, oxonol and rhodamines 700 and 101, because the coupling to low-frequency vibrations broadens the short-wavelength side of the absorption band.

Figure 6 shows a relationship between the 2hwhm and the solvent shift for different chromophores. For 2hwhm, a lower limit seems to exist as a function of the peak shift. For rigid nonpolar polycyclic arenes (3,4-BP, 9,10-ClA, di-*tert*-butylterrylene) a roughly linear dependence between 2hwhm and $\Delta\nu_{max}$ holds:

$$[\text{2hwhm}] = (108 \pm 8) - (0.087 \pm 0.007)\Delta\nu_{max}; \quad N = 3, \quad r = 0.9967 \quad (13)$$

The inhomogeneous width is equal to about 10% of the dispersive solvent shift plus a residual width of ~100 $cm^{-1}$, in accordance with our earlier work.[28,56] Qualitatively, the slope of eq 13 can be explained by the fluctuations in effective numbers of solvent molecules in the closest layer surrounding the chromophore. The residual width of ~100 $cm^{-1}$ is present even in nonpolar aliphatic hydrocarbon matrixes. It is assigned tentatively to repulsive interactions.

The compounds other than polyarenes have broader spectra (Figure 6). The excessive width in dipolar dyes, rhodamines 700 (466 $cm^{-1}$) and 101, oxazine 1, and trans-*iso*-bacteriochlorin (412 $cm^{-1}$) is likely caused by linear Stark effect in frozen-in solvent cavity fields of different magnitude and direction.[28]

The broadening in the oxonol dye (308 $cm^{-1}$) and HIDCI (382 $cm^{-1}$) as compared to cryptocyanine (222 $cm^{-1}$) may stem from the conformational flexibility of the pentamethine chain in the former structures. The trimethine link in cryptocyanine appears to be relatively rigid and exist in a single conformation. Besides its narrow bandwidth, cryptocyanine has one of the largest Debye−Waller factors among cyanine dyes. Another presumably stiff monomethine compound, pseudoisocyanine, has 2hwhm as broad as 764 $cm^{-1}$ (in glycerol/water) (Table 3) owing to a huge multiphonon sideband that reduces the 0−0 transition probability to a mere 1%.[53]

Specific solvation can provide an additional inhomogeneous broadening mechanism, if the H-bridged solute−solvent complexes are subject to structural variations, i.e., in resazurin. The hydrogen bonded complexes can appear as distinct shoulders of the 0−0 band (oxazine 1, resorufin, tetrazine, see Figure 7). After a deconvolution into Gaussians one obtains that the components can be fairly narrow (~200 $cm^{-1}$ for tetrazine). Therefore, the resorufin−ethanol complexes seem to possess a well-defined structure.

For the sake of completeness, the bandwidths in the liquid phase at 293 K are listed in Table 3. At room temperature the 2hwhm is on the average by $2.0 \pm 0.2$ times broader than that in the low temperature solid. Such proportionality means that in the liquid the amplitude of dynamic fluctuations of the electric field and density are approximately by a factor of 2 larger than the static fluctuations in the frozen glass.

Finally, let us recapitulate the main interactions leading to spectral broadening in molecular glasses, according to Figure 6. The interaction between the permanent dipoles that can also be regarded as a linear Stark effect in the cavity and reaction fields produces the strongest spectral inhomogeneity. The nonuniform matrix fields in polar solvents interact also with solute multipoles resulting in a broadening in centrosymmetric guest molecules. The fluctuations of matrix density (polarizability) are responsible for band broadening by means of dispersive effect. Last but not least, there is a residual width of about 100 $cm^{-1}$ occurring even in aliphatic hydrocarbon glasses and for nonpolar chromophores with very small polarizability changes, such as α ($^1L_b$) type transitions of arenes (pyrene)[28] and porphyrins (octaethylporphine, chlorin).[26] At present, we can only speculate that either repulsive forces or bond dipole interactions are responsible for this phenomenon.

**3. Pressure Shifts of Holes in Ethanol Glass Doped with Different Dyes.** The pressure shift coefficient $d\nu/dP$ measured on a hole burned at the absorption maximum depends linearly on absolute vacuum-to-matrix frequency shift $\Delta\nu_{max}$ (Figure 8, Table 4):

$$d\nu_{max}/dP = (-0.036 \pm 0.029) + (6.27 \pm 0.41) \times 10^{-4}\Delta\nu_{max}, \quad N = 13, \quad r = 0.978. \quad (14)$$

The most strongly deviating points of cryptocyanine, HIDCI, the squarene and oxonol dyes, as well as thionine were excluded from the correlation. The slope of eq 14, $6.27 \times 10^{-4}$ GHz $bar^{-1}$ cm or $2.1 \times 10^{-5}$ $bar^{-1}$ is somewhat smaller than the probable value of $2\beta_T$ for glassy ethanol ($3 \times 10^{-5}$ $bar^{-1}$) (see

**TABLE 3: Band Maxima and Widths of Dopants in Ethanol at 6 K[a]**

| dopant | $\nu_{max}$ ($cm^{-1}$) | $\nu_{max} - \nu_0$ ($cm^{-1}$) | 2hwhm ($cm^{-1}$) | fwhm ($cm^{-1}$) | $\frac{\text{hwhm293}}{\text{whm(6)}}$ | $\nu_{max(293)} - \nu_{max(6)}$ ($cm^{-1}$) |
|---|---|---|---|---|---|---|
| | | | Polymethine Compounds | | | |
| pseudoisocyanine $I^{-}$[b] | 20404 | −688 | 764 | | 1.52 | 130 |
| cryptocyanine $I^{-}$ | 14038 | −592 | 222 | 235 | 2.20 | 53 |
| HIDC $I^{-}$ | 15494 | −566 | 382 | 436 | 2.04 | 99 |
| rhodamine 101 $ClO_4^{-}$ | 17235 | −760 | 460 | 594 | 2.17 | 371 |
| rhodamine 700 $ClO_4^{-}$ | 15248 | −982 | 466 | 593 | 1.66 | 210 |
| oxazine 1 $ClO_4^{-}$ | 15366 | −774 | (394) | 461 | (1.54) | 108 |
| thionine $Cl^{-}$ | 16345 | −1435 | 282 | | 2.13 | 216 |
| squarene dye | 15614 | −739 | 204 | 246 | 2.59 | 188 |
| oxonol dye $Na^{+}$ | 14676 | −664 | 308 | 411 | 2.01 | 50 |
| resorufin $Na^{+}$ | 17280 | −310 | 212 | 281 | (3.46) | 32 |
| resazurin $K^{+}$ | 16523 | 331 | 340 | 418 | 2.51 | −150 |
| | | | Polycyclic Aromatic Hydrocarbons | | | |
| 3,4-benzopyrene | 24824 | −441 | 146 | 142 | 1.81 | −16 |
| 9,10-dichloroanthracene | 24741 | −1209 | 218 | 229 | 2.02 | 224 |
| di-*tert*-butylterrylene | 17784 | −1429 | (230) | 260 | (2.87) | 310 |
| cyclohexylbenzo[*k*]fluoranthene | 24450 | | 260 | 254 | | |
| | 24441[c] | | 300 | 313 | | |
| cyclopropylbenzo[*k*]fluoranthene | 23907 | | 226 | 237 | | |
| | | | Tetrapyrrolic Compounds | | | |
| Mg octaethylporphine | 17342 | | 140 | 142 | 2.06 | −87 |
| chlorin | 15811 | −101 | 136 | 141 | 1.75 | −52 |
| *trans-iso*-bacteriochlorin | 17260 | −725 | 412 | 407 | 1.79 | 53 |
| tetra-*tert*-butylporphyrazine | 16229 | −97 | 188 | 195 | 1.77 | −96 |
| | | | Azaarene with n−$\pi^*$ Transitions | | | |
| tetrazine | 18278 | 150 | | | | −275 |
| | 18289[d] | 161 | | 216 | | −286 |
| | 18035[d] | −93 | | 201 | | −32 |

[a] $\nu_{max}$, band maximum; $\nu_{max} - \nu_0$, absolute solvent shift of the band maximum; 2hwhm, double value of the half-width at half-maximum measured at the long-wavelength slope of the band; fwhm, full-width at half-maximum; hwhm(293)/hwhm(6), relative band broadening between 293 and 6 K; $\nu_{max(293)}$-$\nu_{max(6)}$, band shift between 293 and 6 K; approximate values of parameters for bands with shoulders are given in parentheses. [b] In 50% (w/w) glycerol/water, ref 53. [c] 10% (v/v) of cycloheptatriene was added. [d] Parameters of the two Gaussian components of the band.

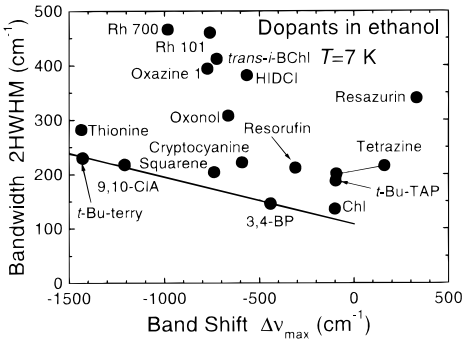


**Figure 6.** Dependence of bandwidth on the vacuum-to-matrix shift of the absorption maximum in ethanol glass at 6 K. For polycyclic hydrocarbons a linear correlation is obtained (eq 13). The remaining compounds have broader bands due to microscopic shift mechanisms other than dispersive forces and/or the conformational flexibility of the structures.

below). In less compressible PMMA matrix the respective numbers are slightly less, $1.8 \times 10^{-5}$ and $2.42 \times 10^{-5}$ $bar^{-1}$.[21]

The pressure shift coefficients of open chain polymethines, irrespective to their charge are anomalously small. With the exception of the neutral squarene, the absolute solvent shifts of band maxima are also considerably less than the expected dispersive red shifts in glassy EtOH (Figure 5). Accordingly, these dyes show hypsochromism in polar liquid solvents (Figure 2a and e).

In protic media the anionic chromophores, resorufin and resazurin have small absolute solvent shifts with respect to the vacuum frequencies of nonsolvated chromophores. The normal dispersive red shift is off-set in hydrogen bonded solute−solvent complexes, so that the maximum of resazurin in solid EtOH is even blue shifted from the vacuum value by 330 $cm^{-1}$. The pressure shift measured at the band maximum is also hypsochromic. Both the resorufin and resazurin obey the correlation (eq 14). Therefore, the influences of compression of the hydrogen bond(s) and that of the increase of matrix polarizability remain balanced under the pressure.

Pressure shifts can be compared with those induced by temperature, as both decompression and thermal expansion increase the intermolecular separation. With the rise of temperature the matrix density decreases, particulary fast in the course of melting, and the Lorentz−Lorenz function $\phi(n^2)$ diminishes from 0.28 to 0.22. This should lead to a decrease of dispersive shift by $p\Delta\phi(n^2) \sim 200$ $cm^{-1}$ in polymethines. This thermal blue shift of band maxima between 6 and 293 K is smaller in cryptocyanine, HIDCI and the oxonol dye (50−100 $cm^{-1}$) (Table 3), reminding the anomaly in *P* shifts. Above the glass transition point the dielectric constant reduces dramatically from 55.5 at 163 K to 25.3 at 293 K (ref 51, p 32). Further, the molecular complexes tend to dissociate as the thermal motions intensify. Both weakening of electrostatic interactions and breaking of hydrogen bonds (in resorufin and resazurin) affect the solvent shifts.

In the following section the dependence of the pressure shifts on hole burning position over the whole spectral contour, rather than just a single value $d\nu_{max}/dP$ will be discussed.

**4. Wavelength Dependence of Pressure Shift Coefficients in EtOH.** The pressure shift coefficients of spectral holes $d\nu/dP$ depend linearly on burning position within the inhomogeneous spectral contour (so-called color effect, refs 7−19) (Figure 7). The linear regression parameters of the plots of $d\nu/dP$ vs the hole burning frequency ($\nu$), i.e., the slope *a* and the frequency at which pressure shift vanishes $\nu_{0(P)}$ are collected in Table 4. Occasionally, a few deviating points at the band edges that could be subject to experimental uncertainties have been excluded

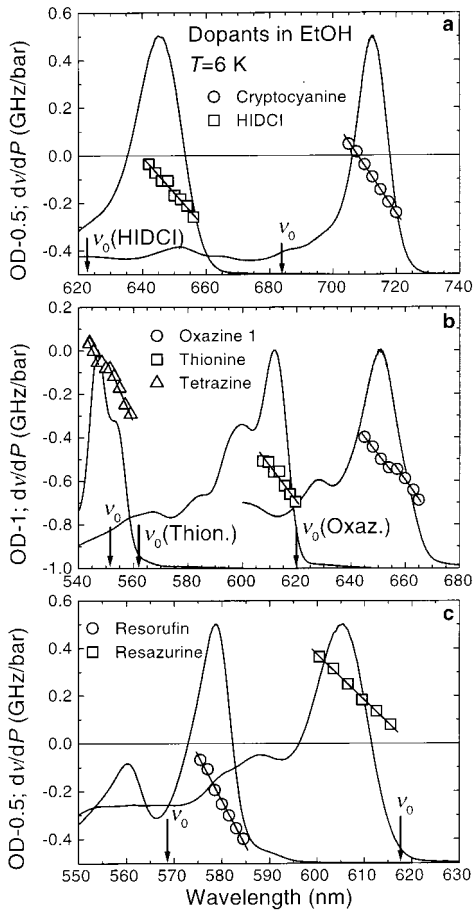


**Figure 7.** Low-temperature absorption spectra and the pressure shift coefficients plotted as a function of hole burning wavelength in ethanol glass for (a) open chain cyanine cations, (b) cyclic polymethine cations and *s*-tetrazine, and (c) cyclic polymethine anions. Oxazine 1 and *s*-tetrazine form two distinct solute−solvent complexes as shown by shoulders in the spectrum and a step in the plot of pressure shift coefficients. The 0−0 origins in nonsolvated chromophores are indicated by arrows.

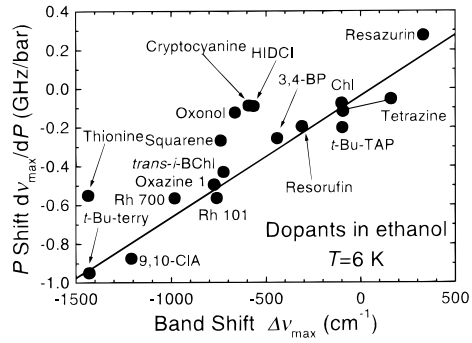


**Figure 8.** Pressure shift coefficients of spectral holes burned at the absorption band maxima (Table 4) plotted as a function of solvent shift in ethanol glass at 6 K. The linear regression line (eq 14) is shown.

from the correlation. Oxazine 1 and *s*-tetrazine form two solvational complexes in ethanol glass distinguishable by the presence of shoulders in the spectrum (Figure 7b). Accordingly, a bilinear relationship d$\nu$/d$P$ vs $\nu$ is obtained with rather similar slopes.

The slope factor $a$ has attracted special interest during the past decade since it has been hoped that it reflects the compressibility of matrix.[7−19] It follows both from the Bakhshiev formula for dispersive shifts (eq 4)[21,22] and simple microscopic models[7,9,20] that (see eq 5)

$$a = 2\beta_T \tag{15}$$

However, inspection of Table 4 reveals that $a$ does not remain constant but varies between $1.5 \times 10^{-5}$ and $6 \times 10^{-5}$ bar$^{-1}$ in a single matrix, solid EtOH. Roughly speaking, it is inversely correlated with inhomogeneous bandwidth (Figure 9):[56]

$$[\text{2hwhm}] = (53 \pm 48) + (623 \pm 124) \times 10^{-5} a^{-1}, \quad N = 18, \quad r = 0.783 \tag{16}$$

In general, broad band spectra have shallow slopes and *vice versa*.

The slopes are particularly shallow in HIDCI ($2.14 \times 10^{-5}$ bar$^{-1}$), rhodamines 101 ($1.69 \times 10^{-5}$ bar$^{-1}$), and 700 ($1.46 \times 10^{-5}$ bar$^{-1}$). As already mentioned, a larger bandwidth of HIDCI with respect to that of cryptocyanine stems from geometrical distortions of $\pi$-electronic system. Provided the conformers with different transition energies (in a vacuum) have similar dispersive shifts, a low value of $a$ would result. In rhodamines the spectra are drastically broadened due to linear Stark effect in the cavity field. Under external pressure the cavity field changes in proportion with linear compressibility $1/3\beta_T$ and so does the hole shift coefficient $a$ (eq 8). Because the slope is small in rhodamines, the extrapolated frequency at which the hole shift vanishes is much higher than the vacuum frequency ($\nu_{0(P)} > \nu_0$). The empirical correlation between 2hwhm and $a^{-1}$ (eq 16) can be easily understood bearing in mind that the Stark effect and the molecular flexibility cause pronounced broadening accompanied by small magnitudes of $a$.

Polycyclic arenes have the highest sensitivity of pressure shifts toward the hole burning wavenumber and the slope factors as large as $(5-6) \times 10^{-5}$ bar$^{-1}$. Also resorufin (4.25), benzo[*k*]fluoranthene derivatives (3.48 and 3.99), squarene dye (3.67), *trans-i*-BChl (3.45), cryptocyanine (3.38), and chlorin (3.34) possess somewhat larger slopes than the probable $2\beta_T$ of EtOH glass (3.0) (all in $10^{-5}$ bar$^{-1}$ units). As in the case of PMMA host matrix, the involvement of repulsive potentials is surmised in order to account for the steep slopes (eq 1).[21] To explain the slope factor of $6 \times 10^{-5}$ bar$^{-1}$, one should make a conjecture that repulsive or some other potential with distance dependence as steep as $r^{-12}$ is responsible for about a half of total band broadening.

A summary of pressure shift coefficients as a function of solvent shifts for polymethines and other chromophores is presented in Figure 10a and b, respectively. For comparison, a linear plot of eq 5 is shown for the probable 2-fold compressibility value of solid EtOH, $2\beta_T = 3 \times 10^{-5}$ bar$^{-1}$. An almost ideal coincidence with eq 5 is observed for resorufin, resazurin, chlorin, *t*-Bu-TAP, as well as the red shifted form of *s*-tetrazine. The data of cryptocyanine, HIDCI, squarene, and oxonol dyes (all open-chain polymethines) lie parallel with the line but are by 0.5 GHz/bar smaller than expected on the basis of $\Delta\nu$.

**5. Analysis of Literature Data.** During the past decade, the behavior of narrow spectral holes under hydrostatic pressure have been recorded in a number of systems, including chromoproteins.[7−19] In Table 5 the slope factors $a$ and the frequencies where the pressure shift vanishes $\nu_{0(P)}$ are collected together with $P$ shift coefficients at the band maxima d$\nu_{max}$/d$P$ as well as the widths and peak positions of the bands under consideration. The references and figures the data are taken from are indicated.

The reported slope factors vary between $1.4 \times 10^{-5}$ and $8.2 \times 10^{-5}$ bar$^{-1}$. The authors generally believe that this way the compressibility is being measured to a good approximation since a test experiment using resorufin, hypericin, protoporphyrin IX,

**TABLE 4: Frequency Dependence of Pressure Shift Coefficients of Spectral Holes in Ethanol at 6 K[a]**

| dopant | $d\nu_{max}/dP$ (GHz/bar) | $\nu_{0(P)}$ ($cm^{-1}$) | $\nu_{0(P)} - \nu_0$ ($cm^{-1}$) | $a$ ($10^{-5}bar^{-1}$) | $N$ | $r$ | data interval (nm) |
|---|---|---|---|---|---|---|---|
| | | | Polymethine Compounds | | | | |
| cryptocyanine $I^-$ | −0.088 | 14127 ± 3 | −503 | 3.38 ± 0.09 | 7 | 0.9984 | 605−620 |
| HIDC $I^-$ | −0.091 | 15617 ± 16 | −443 | 2.14 ± 0.13 | 11 | 0.983 | 642−656 |
| rhodamine 101 $ClO_4^-$ | −0.564 | 18336 ± 89 | 341 | 1.69 ± 0.13 | 5 | 0.9917 | 577−589 |
| rhodamine 700 $ClO_4^-$ | −0.565 | 16503 ± 87 | 273 | 1.46 ± 0.10 | 7 | 0.9894 | 650−668 |
| oxazine 1 $ClO_4^-$ | −0.495 | 16102 ± 32 | −38 | 2.22 ± 0.10 | 4 | 0.9979 | 645−654 |
| | | 15911 ± 56 | −229 | 2.58 ± 0.18 | 4 | 0.9950 | 657−665 |
| thionine $Cl^-$ | −0.550 | 17197 ± 94 | −583 | 2.07 ± 0.22 | 7 | 0.974 | 607.5−619.5 |
| squarene dye | −0.268 | 15851 ± 16 | −502 | 3.67 ± 0.19 | 6 | 0.9946 | 638−648 |
| oxonol dye $Na^+$ | −0.124 | 14806 ± 11 | −534 | 3.21 ± 0.15 | 8 | 0.9933 | 678−692 |
| resorufin $Na^+$ | −0.196 | 17428 ± 8 | −162 | 4.25 ± 0.17 | 7 | 0.9959 | 575.5−584.5 |
| resazurin $K^+$ | 0.275 | 16140 ± 8 | −52 | 2.39 ± 0.06 | 6 | 0.9989 | 600.5−615.5 |
| | | | Polycyclic Aromatic Hydrocarbons | | | | |
| 3,4-benzopyrene[b] | −0.256 | 24966 ± 11 | −229 | 6.19 ± 0.41 | 7 | 0.9891 | 401.5−404.5 |
| 9,10-dichloroanthracene[b] | −0.875 | 25348 ± 33 | −602 | 4.75 ± 0.23 | 6 | 0.9954 | 404−406.5 |
| di-*tert*-butylterrylene | −0.95 | 18743 ± 147 | −470 | 2.83 ± 0.42 | 5 | 0.968 | 560−566 |
| cyclohexylbenzo[*k*]fluoranthene[c] | −0.57 | 24992 ± 20 | | 3.48 ± 0.12 | 8 | 0.9964 | 407.5−411.5 |
| cyclopropylbenzo[*k*]fluoranthene | −0.67 | 24455 ± 34 | | 3.99 ± 0.23 | 7 | 0.9916 | 416.5−421.3 |
| | | | Tetrapyrrolic Compounds | | | | |
| magnesium octaethylporphine | −0.02 | 17378 ± 10 | | 2.03 ± 0.21 | 4 | 0.9890 | 576−580 |
| chlorin | −0.076 | 15885 ± 4 | −27 | 3.34 ± 0.12 | 8 | 0.9960 | 629.5−636.5 |
| *trans-iso*-bacteriochlorin | −0.43 | 17667 ± 41 | −318 | 3.45 ± 0.31 | 7 | 0.980 | 575−586 |
| tetra-*tert*-butylporphyrazine | −0.202 | 16445 ± 9 | 119 | 3.08 ± 0.11 | 6 | 0.9972 | 613.5−621 |
| | | | Azaarenes with n−$\pi^*$ Transitions | | | | |
| tetrazine | −0.054 | 18341 ± 3 | 213 | 2.92 ± 0.21 | 4 | 0.9950 | 544−547 |
| | −0.117 | 18217 ± 10 | 89 | 3.00 ± 0.14 | 5 | 0.9966 | 551.5−559 |

[a] $d\nu_{max}/dP$, pressure shift coefficient at the band maximum; $\nu_{0(P)}$, frequency at which spectral hole shows no shift with pressure change; $\nu_0$, transition frequency of the nonsolvated dopant; *a*, slope of the linear dependence of the pressure shift coefficient on hole frequency; *N*, number of data points; *r*, correlation coefficient. [b] 5% (v/v) of *tert*-butyl perbenzoate was added to enhance hole burning quantum efficiency. [c] 10% (v/v) of cycloheptatriene was added.

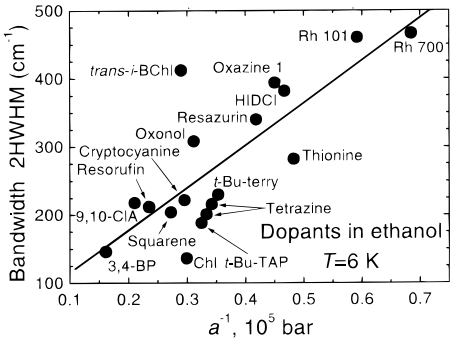


**Figure 9.** Relationship between the bandwidth and the inverted slope factor of pressure shift coefficients vs hole burning frequency in EtOH glass. The slope factor *a* is not a constant equal to 2-fold compressibility of the matrix but decreases with increasing bandwidth. The regression line (eq 16) is shown.

and dimethyl-*s*-tetrazine in ethanol−methanol (3:1 v/v) has yielded indeed very similar slopes of $(3.3 \pm 0.3) \times 10^{-5}$ $bar^{-1}$.[15] However, this assumption is open to doubt, since more extensive sets of probes in ethanol and PMMA[21,56] reveal that the slope factors can vary in a broad range in the same matrix (Figures 9 and 10, Table 4). Also, the agreement between the true vacuum frequencies and $\nu_{0(P)}$ is generally poor.

The band maxima of resorufin shift gradually to the red as the protic character of the matrix diminishes in the order of ethylene glycol/$H_2O$ mixture[9,10] > glycerol[9] > EtOH/MeOH mixture[7] > EtOH (this work) > *n*-butanol/*tert*-butyl alcohol mixture.[12] The bands are clearly not elementary. In *n*-butanol/*tert*-butyl alcohol (Figures 1 and 5 in ref 12) and EtOH (Figure 7c) the spectral components are resolved already in absorption. The plots of $d\nu/dP$ vs $\nu$ reveal two linear segments in glycerol (Figure 7 in ref 9). In glycol/$H_2O$ the *P* shift plot consists, in fact, also of two parts with different slopes (Figure 3 in ref 9). Therefore, the investigation of *P* shifts of holes helps to separate solvational complexes. It may seem likely that lower compressibility of rigid H-bonded network of the glycerol glass is reflected in the lower slope factors (1.6 and 2.1)[9] as compared to those in EtOH/MeOH (3.6),[7] EtOH (4.25, this work, Table 4), and *n*-BuOH/*tert*-BuOH (3.4 and 4.1)[12] (all in $10^{-5}$ $bar^{-1}$ units). However, such a conclusion is premature, since the 2hwhm is tremendously broad in glycerol (820 $cm^{-1}$ [9] vs 212 $cm^{-1}$ in EtOH).

The horseradish peroxidase (HRP) apoprotein combined with non-native cofactors mesoporphyrin IX[11,13,18] and its magnesium complex[19] have been explored by means of hole burning. Several spectral bands of mesoporphyrin IX have been observed between 16100 and 16300 $cm^{-1}$ depending on the pH, the exposure of the system to the light or the complexing with an aromatic substrate, 1-naphthohydroxamic acid.[11,13,16] The highest energy band of mesoporphyrin in HRP ($B_1$ at 16317 $cm^{-1}$ [16]) is nearly as blue shifted as that of hematoporhyrin in water (16431 $cm^{-1}$) (Figure 3). Upon irradiation with light[16] or complexing with 1-naphthohydroxamic acid[11,13] the blue $B_1$ band gives rise to red shifted forms with narrower bandwidths. The holes burned in the broader high-frequency bands have much smaller slope factors ($a = \sim 2.5 \times 10^{-5}$ $bar^{-1}$) than those burned in the narrow low frequency forms ($(6-8) \times 10^{-5}$ $bar^{-1}$). Specific solvation with water is probably responsible for the presence of blue shifted pigment forms in HRP that have relatively large bandwidths and shallow slopes *a*.

The free-base protoporphyrin IX embedded in myoglobin shows, in principle, similar behavior, although the spectra of different forms are poorly resolved.[10,13,14] The respective slope

**TABLE 5: Frequency Dependence of Pressure Shift Coefficients of Spectral Holes at 1.5−4.2 K from Literature**

| dopant | host matrix | $\nu_{max}$[a], ($cm^{-1}$) | 2hwhm[b] ($cm^{-1}$) | $d\nu_{max}/dP$[c] (GHz/bar) | $\nu_{0(P)}$[d] ($cm^{-1}$) | $a$[e] ($10^{-5}bar^{-1}$) | data interval ($cm^{-1}$) | ref | figs |
|---|---|---|---|---|---|---|---|---|---|
| resorufin | ethylene glycol/$H_2O$(1:1v/v) | 17480 | 600 | 0.25 | 17100 | 2.2 | 16950−17600 | 9;10 | 1,3; 1,3 |
| resorufin | glycerol | | | | 17300 | 1.6 | 17270−17570 | 9 | 5,7 |
| | | 17300 | 820 | 0 | 17050 | 2.1 | 16750−17100 | | |
| resorufin | EtOH/MeOH (3:1?) | 17300 | 247 | −0.21 | 17500 | 3.6 | 17170−17470 | 7 | 1,4 |
| resorufin | *n*-butanol/tert-butanol(1:1) | 17236 | 201 | −0.19 | 17390 | 4.1 | 17015−17380 | 12 | 5 |
| | | 16890 | 208 | −0.22 | 17110 | 3.4 | 16730−17065 | | |
| hypericin | ethanol/methanol (3:1) | 16845 | 173 | −0.36 | 17224 | 3.0 | 16760−17040 | 15 | 3 |
| hypericinate anion | glycerol/DMF (3:1 v/v) | 16820 | 273 | −0.30 | 17200 | 2.5 | 16600−17080[f] | 18 | 5 |
| hypericinate anion | HSA[g]complex in glycerol/$H_2O$ (3:1 v/v) | 16730 | 420 | −0.47 | ∼17600 | ∼2.1 | 16300−16600[h] | | 6 |
| mesoporphyrin IX | HRP[i]isoenzyme $C_2$ in | 16317$B_1$ | 97 | −0.17 | 16562 | 2.3 | 16303−16342 | 16 | 1,3 |
| | glycerol/$H_2O$ (1:1 v/v), | 16208$B_2$ | 53 | −0.26 | 16354 | 5.9 | 16190−16225 | | |
| | pH = 8 | 16110$B_3$ | 57 | −0.22 | 16233 | 6.0 | 16080−16138 | | |
| mesoporphyrin IX | same, after photobleaching of $B_1$ | 16207$B_2$ | 61 | −0.27 | 16385 | 4.9 | 16160−16240 | 16 | 4 |
| | | 16108$B_3$ | 61 | −0.22 | 16228 | 6.1 | 16070−16123 | | |
| mesoporphyrin IX | HRP[i] isoenzyme $C_2$ in glycerol/ $H_2O$ (1:1 v/v), pH = 5 | 16308 | 88 | −0.24 | 16592 | 2.7 | 16280−16348 | 11;13 | 4, table; 7 |
| mesoporphyrin IX | same, complex with 1-naphtho- | 16260 | | | | | | 11;13 | 4, table; 7 |
| | hydroxamic acid | 16173 | 67 | −0.38 | 16326 | 8.2 | 16160−16197 | | |
| protoporphyrin IX | EtOH/MeOH (3:1)+ 1%DMF | | | | | 3.0 | | 15 | 4 |
| protoporphyrin IX | glycerol/DMF (3:1 v/v) | 15985 | 185 | 0.063 | 15890 | 2.4 | 15860−16000[j] | 14 | 3 |
| protoporphyrin IX | myoglobin | 16080 | 107[k] | 0.075 | 15920 | 1.6 | 16050−16180 | 10 | 6 |
| | | 15990[l] | | 0.063[m] | 15795 | 1.4 | 15915−15990 | | |
| protoporphyrin IX | myoglobin in glycerol/$H_2O$ | 16100 | ∼185[n] | 0.09[o] | 16087 | 2.5 | 16160−16275 | 13;14 | 6; 2 |
| | (5:2 v/v) | | | 0.12[p] | 15880 | 6.2 | 15760−15880 | | |
| magnesium mesoporphyrin | EtOH/glycerol (1:1 v/v) | 17315 | ∼240 | −0.41 | 17370 | 2.0 | 17230−17390 | 19 | 8, text |
| magnesium | HRP[i] isoenzyme C in glycerol/ | 17160[q] | | −0.435 | 17830 | 2.12 | 17160−17240 | 19 | 1,6, text |
| mesoporphyrin | $H_2O$ (1:1), pH = 7 | 17063 | 53[r] | −0.315 | 17570 | 2.1 | 16980−17085 | | |
| magnesium mesoporphyrin | same, complex with 1-naphtho- hydroxamic acid | 17150 | 64 | −0.40 | 17655 | 2.6 | 17115−17180 | 19 | 7, text |
| chlorin | benzophenone glass | 15730 | 238 | −0.27 | 16030 | 2.9 | 15570−15870 | 17 | 5, text |
| dimethyl-*s*-tetrazine | EtOH/MeOH (3:1) | | | | | 3.3 | | 15 | 4 |

[a]Absorption maximum. [b]Double value of the half-width at half-maximum of the red side of the band. [c]Pressure shift coefficient of the hole burned at the band maximum. [d]Frequency at which pressure shift vanishes. [e]Slope of the linear dependence of pressure shift coefficient vs the hole burning frequency. [f]Low-frequency portion was left out. [g]Human serum albumine. [h]Low-frequency slope of the band. [i]Horseradish peroxidase. [j]High-frequency portion was left out. [k]2hwhm of the high-frequency side of the band. [l]Low-frequency shoulder. [m]At 15950 $cm^{-1}$. [n]Full width at half-maximum of an asymmetric band. [o]At 16220 $cm^{-1}$. [p]At 15820 $cm^{-1}$. [q]The $S_2-S_0$ transition. [r]The reported width of IDF is 40 ± 5 $cm^{-1}$.

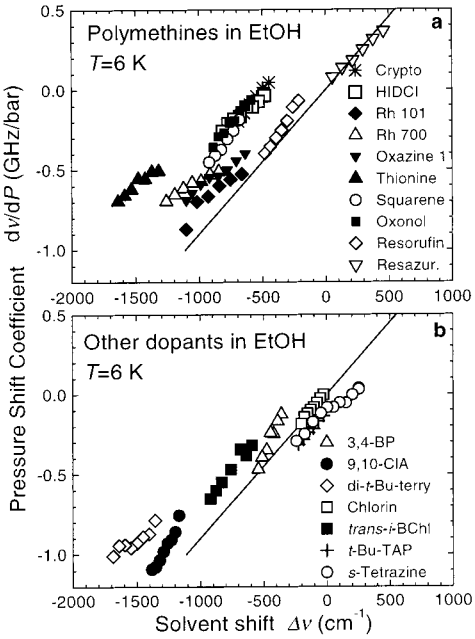


**Figure 10.** Pressure shift coefficients of spectral holes plotted as a function of absolute solvent shifts. The holes are burned over the inhomogeneous bands of polymethine dyes (a) and polycyclic arenes, tetrapyrroles and *s*-tetrazine (b) in ethanol glass. For comparison lines are drawn that pass zero and have a slope of $3 \times 10^{-5}$ $bar^{-1}$, the probable double compressibility value of ethanol glass.

factors can be associated with different solvent shift mechanisms rather than dramatic changes in local compressibility of the protein host matrix.

## Conclusions

In the literature, the pressure induced shifts of zero-phonon holes burned over the inhomogeneous band have been used for determination of two essential parameters: matrix compressibility $\beta_T$ and transition energy of the nonsolvated chromophore $\nu_0$.[7−19] Our previous study in polymer host matrixes[21,56] and the present investigation in solvent glasses have revealed more complex nature of hole shifts under the pressure. Because a linear relationship between the pressure shift coefficients $d\nu/dP$ and the hole position is observed in most cases, a question arises about the physical meaning of the slopes and intercepts of these plots as far as they fail to give $2\beta_T$ and $\nu_0$ directly.

In this work the shifts of spectral holes burned in the 0−0 bands of 20 chromophores doped in single host, glassy ethanol are examined. The slope factor $a$ remains by no means constant in EtOH, but decreases as the inhomogeneous bandwidth increases. Nearly a half of the dopants, including *t*-Bu-TAP, shows the slope values clustering around $3 \times 10^{-5}$ $bar^{-1}$. This corresponds perhaps to the double compressibility of the matrix, since a nice agreement between the slope factor and $2\beta_T$ has been found for isotropic polymers doped with *t*-Bu-TAP.[21] The slope equal to $2\beta_T$ is expected for dispersive interaction that obeys the distance dependence $r^{-6}$. The slope $2\beta_T$ follows directly from Bakhshiev equation (eq 4), since the matrix polarizability increases and the Onsager volume decreases when pressure is applied.[21]

The solvent shift in polycyclic hydrocarbons is mainly of dispersive origin.[22,23,25] Therefore, it has been puzzling to find that the sensitivity of $P$ shift coefficients vs the burning wavelength can be steeper than $2\beta_T$ of the polymer host matrix.[21] For 3,4-benzopyrene and 9,10-dichloroanthracene in EtOH the

slopes are also nearly two times higher than the probable value of $2\beta_T$. We have suggested, that the most plausible cause of such an increase stems from the repulsive forces between the molecules that may have the intermolecular distance dependence as steep as $r^{-12}$. Accordingly, there is a residual inhomogeneous bandwidth of about 80−100 $cm^{-1}$ in nonpolar polymers and solvent glasses,[28] even in symmetric porphyrins having no dipole moment and a very small polarizability change upon the $S_1-S_0$ excitation. This residual broadening could be ascribed to the inhomogeneity of repulsive interactions in disordered hosts.

The slopes smaller than $2\beta_T$ could be assigned to the electrostatic interactions of dipolar molecules, such as rhodamines and oxazine 1 in the matrix cavity fields. The strength of a cavity field is proportional to the linear compressibility of the matrix yielding $a$ as small as $1/3\beta_T$. Conformational flexibility of $\pi$-electronic chains (e. g. in HIDCI as compared to cryptocyanine) may provide another broadening mechanism with concomitant low slope factor.

Another category (besides repulsive forces) of intermolecular interactions uncovered and characterized in this study causes hypsochromism of many centrosymmetric chromophores in polar environments. This blue shift in cationic and anionic open-chain polymethines and *s*-tetrazine may be tentatively ascribed to the orientation of solvent dipoles by the local charges of the dye creating a multipolar reaction field that in its turn influences the electronic transition energy. However, the pressure shifts of spectral holes demonstrate, that the microscopic mechanism of this hypsochromic behavior is not uniform.

Obviously, no single method would provide us with sufficient knowledge about intermolecular potentials in the ground and the excited states that extend over a wide range of distances. The fairly complex solvent shift phenomena should be carefully disentangled using simultaneously the matrix, pressure, temperature, and electric field effects on the levels of single chromophores, energy selected ensembles addressed by hole burning, and broad bands.

**Acknowledgment.** I thank Professor Urs P. Wild for continuous support and encouragement during my stay in Physical Chemistry Laboratory, Swiss Federal Institute of Technology (ETHZ), CH-8092 Zürich, Switzerland, where the measurements were performed. I am very grateful to Bruno Lambillotte and Roland Schmidli (ETHZ) for the help in designing the pressure cell and its skilful machining. This work was supported in part by the Board of the Swiss Federal Institutes of Technology, ETHZ, and the Estonian Science Foundation Grant N 3869.

## References and Notes

(1) Koppel, I. A.; Palm, V. A. In *Advances in Linear Free Energy Relationships*; Chapman, N. B., Shorter, J., Eds.; Plenum Press: London, 1972; pp 203−280.
(2) Weigang, O. E., Jr.; Robertson, W. W. In *High-Pressure Physics and Chemistry*; Bradley, R. S., Ed.; Academic Press: London, 1963; Vol. 1, pp 177−205.
(3) Zipp, A.; Kauzmann, W. *J. Chem. Phys*. **1973**, *59*, 4215.
(4) Okamoto, B. Y.; Drickamer, H. G. *J. Chem. Phys*. **1974**, *61*, 2870.
(5) Drickamer, H. G. *Annu. Rev. Phys. Chem*. **1982**, *33*, 25.
(6) Sesselmann, Th.; Richter, W.; Haarer, D.; Morawitz, H. *Phys. Rev. B*. **1987**, *36*, 7601.
(7) Gradl, G.; Zollfrank, J.; Breinl, W.; Friedrich, J. *J. Chem. Phys*. **1991**, *94*, 7619.
(8) Zollfrank, J.; Friedrich, J.; Fidy, J. Vanderkooi, J. M. *J. Chem. Phys*. **1991**, *94*, 8600.
(9) Zollfrank, J.; Friedrich, J. *J. Phys. Chem*. **1992**, *96*, 7889.
(10) Zollfrank, J.; Friedrich, J. *J. Opt. Soc. Am. B*. **1992**, *9*, 956.
(11) Fidy, J.; Vanderkooi, J. M.; Zollfrank, J.; Friedrich, J. *Biophys. J*. **1992**, *63*, 1605.
(12) Schellenberg, P.; Friedrich, J. *J. Lumin*. **1993**, *56*, 143.
(13) Gafert, J.; Friedrich, J.; Parak, F.; Fidy, J. *J. Lumin*. **1993**, *56*, 157.
(14) Gafert, J.; Friedrich, J.; Parak, F. *J. Chem. Phys*. **1993**, *99*, 2478.
(15) Pschierer, H.; Friedrich, J.; Falk, H.; Schmitzberger, W. *J. Phys. Chem*. **1993**, 97, 6902.
(16) Friedrich, J.; Gafert, J.; Zollfrank, J.; Vanderkooi, J.; Fidy, J. *Proc. Natl. Acad. Sci*. **1994**, *91*, 1029.
(17) Schellenberg, B.; Friedrich, J.; Kikas, J. *J. Chem. Phys*. **1994**, *100*, 5501.
(18) Köhler, M.; Gafert, J.; Friedrich, J.; Falk, H.; Meyer, J. *J. Phys. Chem*. **1996**, *100*, 8567.
(19) Balog, E.; Kis-Petik, K.; Fidy, J.; Köhler, M.; Friedrich, J. *Biophys. J*. **1997**, *73*, 397.
(20) Laird, B. B.; Skinner, J. L. *J. Chem. Phys*. **1989**, *90*, 3274.
(21) Renge, I. *J. Phys. Chem. A* **2000**, *104*, 3869.
(22) Bakshiev, N. G.; Girin, O. P.; Piterskaya, I. V. *Opt. Spektrosk*. **1968**, *24*, 901 (*Opt. Spectrosc*. **1968**, *24*, 483).
(23) Renge, I. *Chem. Phys*. **1992**, *167*, 173.
(24) Renge, I.; van Grondelle, R.; Dekker: J. P. *J. Photochem. Photobiol., A* **1996**, *96*, 109.
(25) Renge, I. *J. Photochem. Photobiol. A* **1992**, *69*, 135.
(26) Renge, I. *J. Phys. Chem*. **1993**, *97*, 6582.
(27) Renge, I.; Wolleb, H.; Spahni, H.; Wild, U. P. *J. Phys. Chem*. **1997**, *101*, 6202.
(28) Renge, I.; Wild, U. P. *J. Lumin*. **1996**, *66&67*, 305.
(29) Spencer, G. H., Jr.; Cross, P. C.; Wiberg, K. B. *J. Chem. Phys*. **1961**, *35*, 1925.
(30) Renge, I. *J. Chem. Phys*. **1997**, *106*, 5835.
(31) Greenblatt, G. D.; Nissani, E.; Zaroura, E.; Haas, Y. *J. Phys. Chem*. **1987**, *91*, 570.
(32) Hirayama, S.; Iuchi, Y.; Tanaka, F.; Shobatake, K. *Chem. Phys*. **1990**, *144*, 401.
(33) Even, U.; Jortner, J. *J. Chem. Phys*. **1982**, *77*, 4391.
(34) Smalley, R. E.; Wharton, L.; Levi, D. H.; Chandler, D. W. *J. Chem. Phys*. **1978**, *68*, 2487.
(35) *Persistent Spectral Hole-Burning: Science and Applications*; Moerner, W. E., Ed.; Springer: Berlin, 1988.
(36) *Single-Molecule Optical Detection, Imaging and Spectroscopy*; Basché, T., Moerner, W. E., Orrit, M., Wild, U. P., Eds.; VCH: Berlin, 1996.
(37) Wallenborn, E.-U.; Wild, U. P.; Brown, R.*J. Chem. Phys*. **1997**, *107*, 8338.
(38) Cichos, F.; Brown, R.; Rempel, U.; von Borczyskowski, C. *J. Phys. Chem*. **1999**, *103*, 2506.
(39) McCarty, M., Jr.; Robinson, G. W. *Mol. Phys*. **1959**, *2*, 415.
(40) Sverdlova, O. V.; Bakhshiev, N. G. *Opt. Spektrosk*. **1977**, *42*, 288.
(41) Jones, P. F. *J. Chem. Phys*. **1968**, *48*, 5448.
(42) Longuet-Higgins, H. C.; Pople, J. A. *J. Chem. Phys*. **1957**, *27*, 192.
(43) Böttcher, C. J. F. *Theory of Electric Polarization*; Elsevier: Amsterdam, 1973; Vol. I.
(44) Marcus, R. A. *J. Chem. Phys*. **1965**, *43*, 1261.
(45) Nicol, M.; Swain, J.; Shum, Y.-Y.; Merin, R.; Chen, R. H. H. *J. Phys. Chem*. **1968**, *48*, 3587.
(46) Ghoneim, N.; Suppan, P. *Spectrochim. Acta A*, **1995**, *51*, 1043.
(47) Renge, I. *J. Opt. Soc. Am. B* **1992**, *9*, 719.
(48) Palm, V. A. *Fundamentals of Quantitative Theory of Organic Reactions*; Khimiya: Leningrad, 1977 (in Russian).
(49) *Aldrich Catalog Handbook of Fine Chemicals 1994−1995*; Aldrich Chemical Co., Inc.: Milwaukee, WI, 1994.
(50) Laurence, C.; Nicolet, P.; Dalati, M. T.; Abboud, J.-L. M.; Notario, M. *J. Phys. Chem*. **1994**, *98*, 5807.
(51) *Landolt-Börnstein. Zahlenwerte und Funktionen*; New Series IV; Springer: Berlin, 1991; Part 6.
(52) Weast, R. C., Ed. *Handbook of Chemistry and Physics*, 52nd ed.; The Chemical Rubber Co: Ohio, 1971−1972; p D-191.
(53) Renge, I.; Wild, U. P. *J. Phys. Chem*. **1997**, *101*, 7977.
(54) Dubinin, N. V.; Blinov, L. M.; Yablonskii, S. V. *Opt. Spektrosk*. **1978**, *44*, 807 (*Opt. Spectrosc*. **1978**, *44*, 473).
(55) Johnson, L. W.; Murphy, M. D.; Pope, C.; Foresti, M.; Lombardi, J. R. *J. Chem. Phys*. **1987**, *86*, 4335.
(56) Renge, I.; Wild, U. P. *J. Lumin*. **2000**, *86*, 241.